

Article

A Success Story in Controlling Sand and Dust Storms Hotspots in the Middle East

Ali Al-Dousari ^{1,*} , Ali Omar ², Ali Al-Hemoud ¹, Abdulaziz Aba ¹, Majid Alrashedi ³ , Mohamad Alrawi ⁴, Alireza Rashki ⁵ , Peter Petrov ¹, Modi Ahmed ¹, Noor Al-Dousari ¹, Omar Baloshi ¹, Meshael Jarba ¹, Ala Esmail ³, Abeer Alsaleh ¹ and Teena William ¹

¹ Environment & Life Sciences Research Center, Kuwait Institute for Scientific Research, Kuwait City P.O. Box 24885, Kuwait

² NASA Langley Research Center, Hampton, VA 23681-2199, USA

³ Energy & Building Research Center, Kuwait Institute for Scientific Research (KISR), Kuwait City P.O. Box 24885, Kuwait

⁴ Geography Department, Aswan University, Aswan P.O. Box 81528, Egypt

⁵ Desert and Arid Zones Management Department, Ferdowsi University of Mashhad, Mashhad P.O. Box 91775-1111, Iran

* Correspondence: adousari@kisar.edu.kw

Abstract: Using 30 years of satellite observations, two sand and dust storms (SDS) source locations (hotspots) were detected on the southern side of the Mesopotamian Flood Plain. Around 40 million people in the region are affected by the two hotspots, including populations in Iraq, Iran, Kuwait, Saudi Arabia, Qatar, Bahrain, and Emirates. Both hotspots encompass roughly 8212 km² and contribute 11% to 85% in 2005 and 2021, respectively, of the total SDS in the region. Dust physical (particle surface area and size percentages) and chemical (mineralogy, major and trace elements, and radionuclides) properties show close similarities between source and downwind samples during SDS originated solely from the two hotspots. Deposited dust size particles show a finning trend towards the north in the Middle East compared to the south. A comprehensive assessment of the chemical and physical properties of soil and dust samples was conducted as an essential step in developing and implementing a mitigation plan in order to establish a success story in reducing SDS, improving air quality, and benefiting the gulf countries and neighboring regions.

Keywords: climate change; dust; sand and dust storms; hotspot; Iraq; Iran; Kuwait; UAE; Middle East



Citation: Al-Dousari, A.; Omar, A.; Al-Hemoud, A.; Aba, A.; Alrashedi, M.; Alrawi, M.; Rashki, A.; Petrov, P.; Ahmed, M.; Al-Dousari, N.; et al. A Success Story in Controlling Sand and Dust Storms Hotspots in the Middle East. *Atmosphere* **2022**, *13*, 1335. <https://doi.org/10.3390/atmos13081335>

Academic Editors: Avelino Eduardo Saez and Pavel Kishcha

Received: 23 June 2022

Accepted: 15 August 2022

Published: 22 August 2022

Publisher's Note: MDPI stays neutral with regard to jurisdictional claims in published maps and institutional affiliations.



Copyright: © 2022 by the authors. Licensee MDPI, Basel, Switzerland. This article is an open access article distributed under the terms and conditions of the Creative Commons Attribution (CC BY) license (<https://creativecommons.org/licenses/by/4.0/>).

1. Introduction

A sand and dust storms (SDS) hotspot can be defined as a spot location where SDS originated from or near surroundings [1]. It is not specifically a certain point location, but more similar to a polygon area. In the Middle East, the unusual meteorological conditions with extremely dry and hot environments enhance very fine sand, clay, and silt particles for erosion during sand and dust storms in the region. Key features of a dust hotspot are a desert environment, strong winds, loose, fine sediments, and rare or absent vegetation. Elevated terrain in the region coupled with strong winds accelerates the transport of the dust from hotspots over a wide geographic region. SDS has profound impacts beyond local and regional limits, making them a global issue. Dust particles resulting from wind erosion make up half of the aerosols in the troposphere [2]. The dry regions of Northern Africa, Middle East, Central Asia, and China, as well as America, South Africa, and to a lesser extent Australia, are the primary suppliers of worldwide mineral dust [2,3]. In the desert ecosystem, the wind is the most active element, which has the ability to blow away sand, silt, and clay-sized particles from the surface over great distances via SDS [1]. Dust is categorized based on visibility (vis) into blowing dust (vis between 1 and 5 km), suspended dust (vis < 10 km), and SDS (vis below 1 km) [4].

Globally, the Middle East has one of the highest fluxes of fallen dust [5–7]. The SDS is a persistent challenge in the Middle East Region. The dust fluxes depend on the severity, time extent, loftiness, and distance from the origin [8]. The Mesopotamian Flood Plain, Iraq's Western Desert, northern Africa's Sahara, and the Nafud and Empty Quarter Deserts are the main sources of silica dust in the Middle East [9]. The regional SDS is a precarious event interacting with exposure circumstances, capacity, and vulnerability, resulting in a socioeconomic negative effect on the region [2]. Such events have a wide range of negative consequences, ranging from economic disruptions to serious health consequences for the population. Dust concentrations in the environment have an extensive effect on human health. The dust particle size is a crucial indicator of possible health risks. Particles bigger than 10 μm in diameter are not easily inhaled, and therefore, they can harm external tissues and organs, causing eye infections and skin irritations [10]. Allergy, asthma, tracheitis, silicosis, and pneumonia are all connected with particles of sizes less than 10 μm , which are easily breathable and are frequently stuck in the throat, mouth, nose, and upper part of the respiratory system. The tiniest dust grains with a diameter of less than 2.5 μm can pass through the lower part of the respiratory system and into the circulation, where they are able to harm all internal tissues or organs and cause heart problems [11]. According to a 2014 worldwide model evaluation within over 30 populations, dust grains with a diameter less than 2.5 μm caused nearly 400,000 untimely deaths due to cardiovascular illness [12].

The Middle East mainly consists of deserts and is affected by SDS throughout the year [13]. Climate change, soil formation, loess deposition, ocean sedimentation, and nutrient inputs to marine and terrestrial ecosystems are all examples of SDS ecological impacts. Additionally, the SDS is transporting microorganisms (viruses, fungi, bacteria, pollen, and spores). Microorganisms associated with dust, in particular, can have a direct influence on human health through pathogenesis, sensitivity development (e.g., asthma) as a result of continuous exposure, and cellular component exposure (pollen and fungal allergens, for example) [10]. In arid areas, dust storms are the most dangerous natural hazard, commonly occurring in the Middle East's environment, and are considered a characteristic feature of the environment. The transportation of dust poses a variety of risks to human civilization [14]. These include effects on air quality, radiative transfer, and ecological impacts.

Preventing and mitigating desertification in locations where sand and dust storms originate, such as southern Iraq, is necessary to reduce SDS incidents in the Middle East. Similarly, efforts should be implemented in the Middle East to diminish the impact of SDS and the numerous challenges they generate. Meteorological conditions and soil characteristics in hotspot areas for local and global are the driving forces of SDS. Precise SDS paths for each season were identified by previous studies [15–19], and it was determined that the prevailing northern winds from Syria and southern Iraq are the primary suppliers of SDS that occur between February and April [20], with a dust fallout rate to maximum more than 400 $\text{tons}\cdot\text{km}^{-2}\cdot\text{yr}^{-1}$ in Ahvaz, southern Iraq, and Kuwait, and the lowest (less than 50 $\text{tons}\cdot\text{km}^{-2}\cdot\text{yr}^{-1}$) in Syria, Lebanon, and Jordan [20]. Deposited dust particles are finer in size fractions on the northern side of the Middle East compared to the southern side. Blown dust is distinguished by its high particulate matter (PM) intensity, which raises dust particle concentrations for a number of days. Severe SDS paths originate from the two main hotspot areas located in the southern part of the Mesopotamian Flood Plain and these paths extend downwind to regions crossing borders and covering southern Iraq, southeastern Iran, Kuwait, eastern Saudi, Qatar, Bahrain, and Emirates. Recently, around 40 million people in the region were shown to be affected by these two hotspots. The aim of this study is to expand the knowledge and awareness of factors and conditions that enable SDS, their effects, and prevention to initiate a success story via setting a mitigation plan to fix SDS hotspot areas on the southern side of the Mesopotamian Flood Plain.

2. Study Area

The two studied areas are in southern Iraq and northern Kuwait, areas (A) and (B), which are 6446 km² and 1181 km², respectively, in 2021 (Figure 1). Both hotspots were identified using satellite images by detecting dust storms for 21 years (2003–2021). The satellite data and images were utilized in tracing minor and major SDS originating from the regional scale. The two SDS hotspots were located not in a certain spot, but in the center of a polygon area where dust originated from. The SDS hotspots Digital Elevation Model (DEM) for both hotspots show lower topography towards the south (Figure 2a) and are covered mostly by loamy sand (Figure 2b). Multiple field visits to the SDS hotspots show bare land with no vegetation and act as the main source of clay and silt particles, which represents the most preferable to be shifted by the wind in the form of dust (Figure 3).

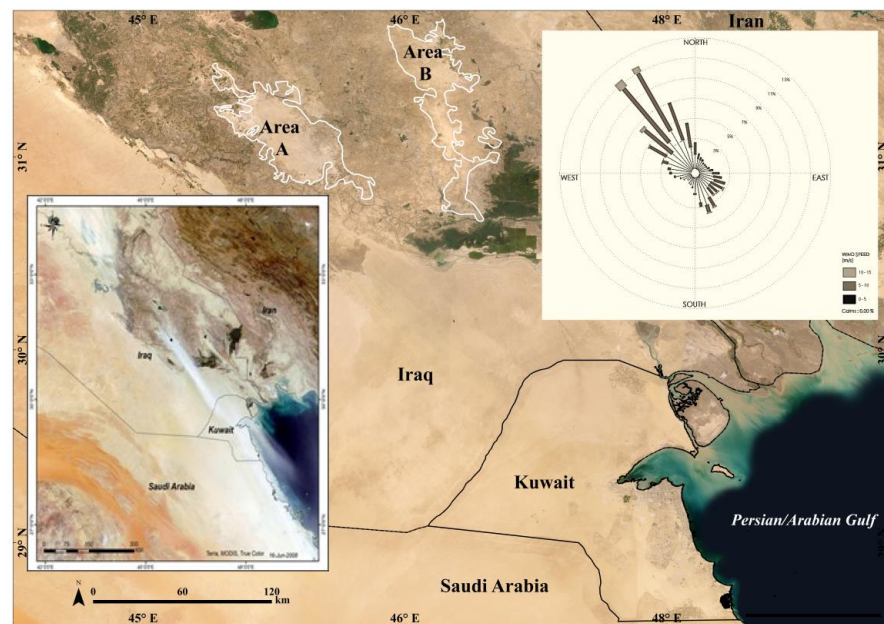


Figure 1. Recent two MODIS images showing the two sand and dust storms hotspots with wind rose from Kuwait City (2000–2020).

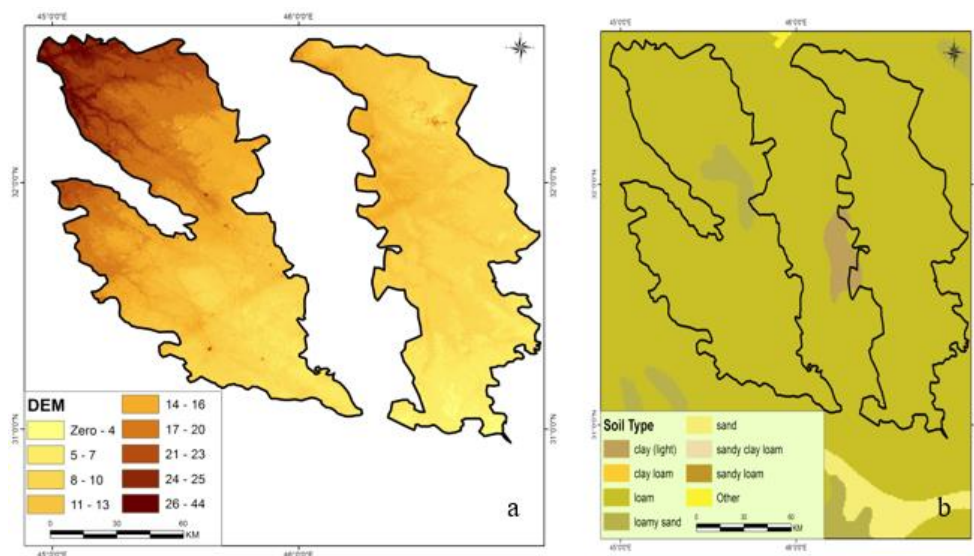


Figure 2. (DEM), SRTM 30meters, USGS (a) and soil map (b).



Figure 3. The hotspot area-A sediments are composed of silty sand and bare vegetation.

3. Materials and Methods

Meticulously, dust samples from building roofs (>10 m) were collected within the study area and surrounding areas and compared to various parts of the world samples to detect regional and worldwide variants in silica dust mineralogical and physical features. These include Um Qasir-Iraq, Manama-Bahrain, Qatar, the western (Wadi Dawasir) and eastern borders of the Empty Quarter Desert (Dubai and Ain at UAE), Amman-Jordan, Cairo-Egypt, and Dushanbe-Tajikistan (Figure 4). In addition, the monthly and annual rates of deposited dust were monitored in Kuwait (located downwind of the two main SDS hotspots using 42 dust traps with 1008 as a total sample for two years from 1st of September to 31st of August for comparison, following the design of [21,22] and later modified by several researchers [15,23]. Around thirty surface sediment samples in a line transect from upwind to downwind were collected from the hotspot (A) during 20–26 April 2019 covering the borders and center of the hotspot area.



Figure 4. Deposited dust sampling locations in the Middle East.

A laser granulometric analyzer was used to estimate particle size percentages. The BET (Brunauer, Emmett, and Teller equation) surface area is measured in this study using Coulter SA 3100 and is represented in terms of values for a certain weight of loose particles in terms of m^2g^{-1} . The samples were softly crushed and examined using the Philips PW-1830 Powder Diffractometer X-ray diffraction (XRD), and using the X'Pert II program, the output data were semi-quantitatively calculated.

The dust samples were prepared in a vial counting geometry for radioactivity measurements. The total net dry weight ranges between 15 g and 0.5 g, kept in a small vial (3 cm length and 1 cm diameter) and stored for about three weeks to achieve the materialistic stability between the ^{222}Rn and its progenies ^{214}Pb and ^{214}Bi for determining the ^{226}Ra content. The prepared samples were counted by a gamma spectrometry system with an exceptionally low energy resolution Canberra Broad Energy Germanium (BEGe) detector (FWHM @ 122 keV is 750 eV). The sample counting time was long enough to get an excellent statistical peak area. The massic activities of the natural radionuclides (^{40}K , ^{224}Ra , ^{226}Ra , ^{228}Ra , and ^{234}Th) and ^{137}Cs were determined using certified calibration standard sources.

The satellite imagery data (Table 1) was collected from multi-sensors from different sources. The atmospheric correction (AC) process for remote sensing is a method of removing the atmospheric effects on the image reflectance values taken by satellite sensors. For removing the effects of the atmosphere using the radiometric calibration tool in ENVI software to calibrate image data to radiance and reflectance. The Normalized Difference Vegetation Index (NDVI) is calculated for the record period from 1984 to 2020 as the difference between the difference and the sum of the refracted near-infrared and red radiations to find change detection for vegetation cover in the two SDS hotspots. The AERONET measurements and MODIS satellite imagery for the sun photometers at Kuwait University in east Kuwait ($29^\circ 19.5' \text{ N}$, $47^\circ 58.3' \text{ E}$) are attained from the AERONET (<https://aeronet.gsfc.nasa.gov> (accessed on 15 June 2022) web page.

Table 1. The list of satellite imagery data that were used in this study.

Sensor Type	Date	Resolution	Sources
Corona satellite	5 May 1968	1 m	https://corona.cast.uark.edu/
Landsat TM	16 May 1984	30 m	https://eos.com/landviewer/
Landsat TM	4 May 1991	30 m	https://eos.com/landviewer/
Landsat ETM +	4 May 2000	30 m	https://eos.com/landviewer/
Landsat OLI	7 April 2013	30 m	https://eos.com/landviewer/
Landsat OLI	10 May 2020	30 m	https://eos.com/landviewer/
Topog Maps	1990	1:200,000	https://maps.vlasenko.net/

4. Results and Discussion

The SDS shape and size are principally controlled by two key elements: the wind (direction and speed) and topography. There are other SDS classifications that depend on visibility, wind seed [19], and particulate matter (PM10) [24]. On the other hand, the SDS dimensions (width and length) are a key factor as larger scale SDS can affect wider areas than the short one. Therefore, this study takes into consideration to put a special classification depending on SDS dimensions. There were 178 SDS events were detected from 19th March 2003 to 13th June 2021 by meteorological stations in the region. Thus, the satellite images of the 178 SDS events were collected in the region. Each SDS dimensionally has a short (maximum width) and a long (maximum length) axis in its mature form the hotspot to the end. In reference to the short axis (the width), there are three main forms of SDS in the Middle East; namely: small, intermediate, and extensive. Among the three main SDS, there are 12 minor forms of sand and dust storms (Figure 5) as follows:

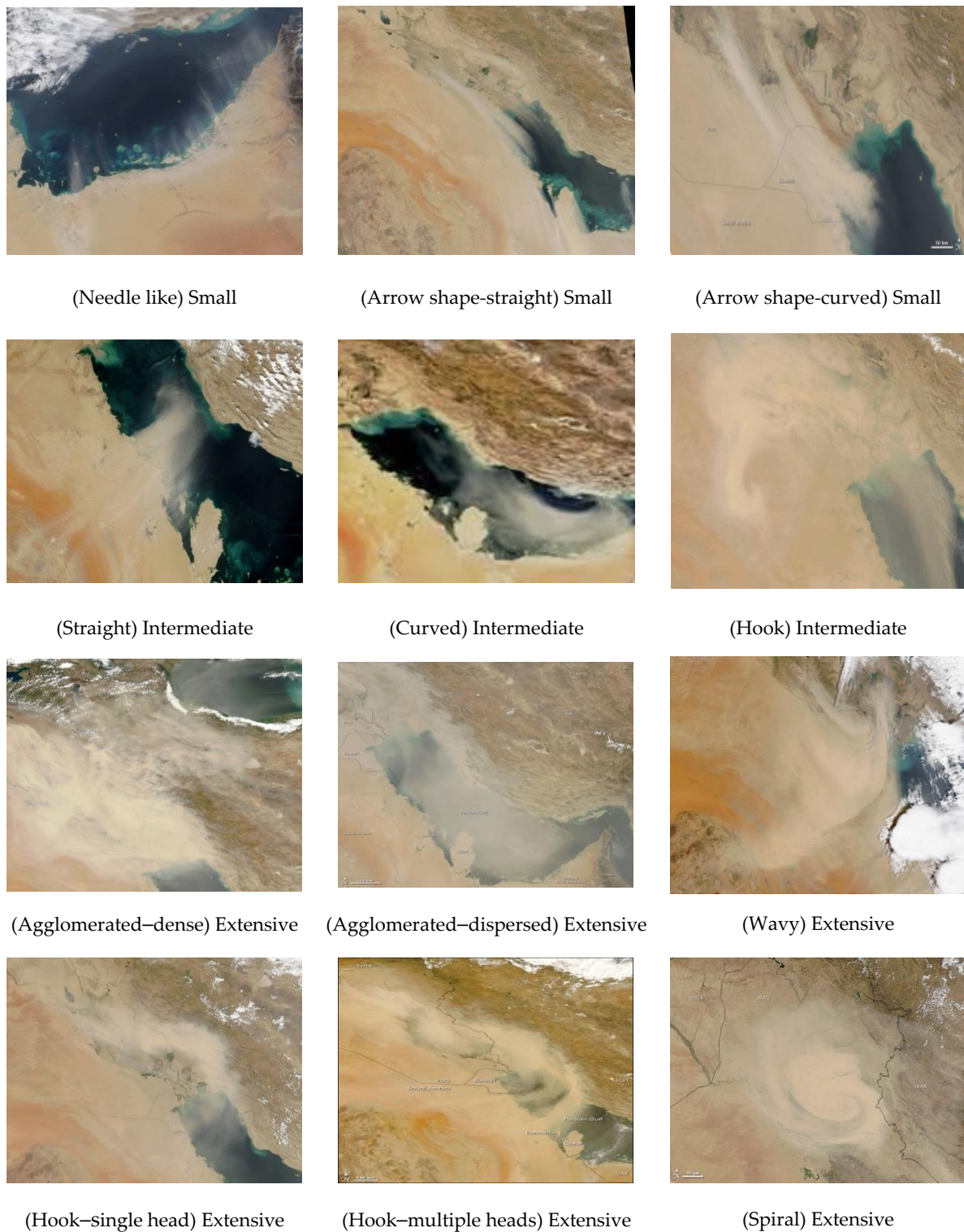


Figure 5. Sorting record of SDS in reference to sand and dust storms width (3 main form types containing 12 sub-forms).

1. Small (with width <100 km from the core of the SDS).
 - a. Has three sub-forms (needle-like, arrow shape-straight, and arrow shape-curved).
2. Intermediate (300–100 km width),
 - a. Has three sub-types (straight, curved, and hook)
3. Extensive (SDS with 300 km width or more)

- a. Encloses six sub-forms (agglomerated–dispersed, agglomerated–dense, wavy, hook–multiple heads, and Spiral Hook–single head),

NASA’s Terra, MODIS (Moderate Resolution Imaging Spectroradiometer) satellite displays brown areas where plants were growing less than they did on average between 2000 and 2008. The MODIS image shows the deterioration of vegetation in the south including the two hotspot areas. Compared to African (Saharan) dust, Arabian dust has multiple sources. The source that has the highest AODs in the Eastern Province of Saudi Arabia, followed by the Nafud desert. The dust characteristics measurements made by CALIPSO are reliable, and the record length is considerable both seasonally and inter-annually. Measurements are useful for assimilation (into) and validation of dust transport models. CALIOP Monthly Mean Dust Aerosol Optical Depth 532 nm, All-sky at night, 2006–2019 (Figure 6a). CALIPSO monitored the vertical distribution of dust plumes downwind of the two hotspots on a regular basis. The dust stretched from the surface to a height of 6 km near Kuwait City, according to the vertical feature mask (Figure 6b,c). The development of dust microphysical characteristics was studied using the volume depolarization ratio, which was shown to rise with longitude, indicating a steady change in dust properties as it moved westward. The total attenuated backscatter CALIPSO observation on 8 July 2019, at night, shows a small arrow curved type of SDS from the area (A) towards Kuwait and the northern Arabian Gulf (Figure 7).

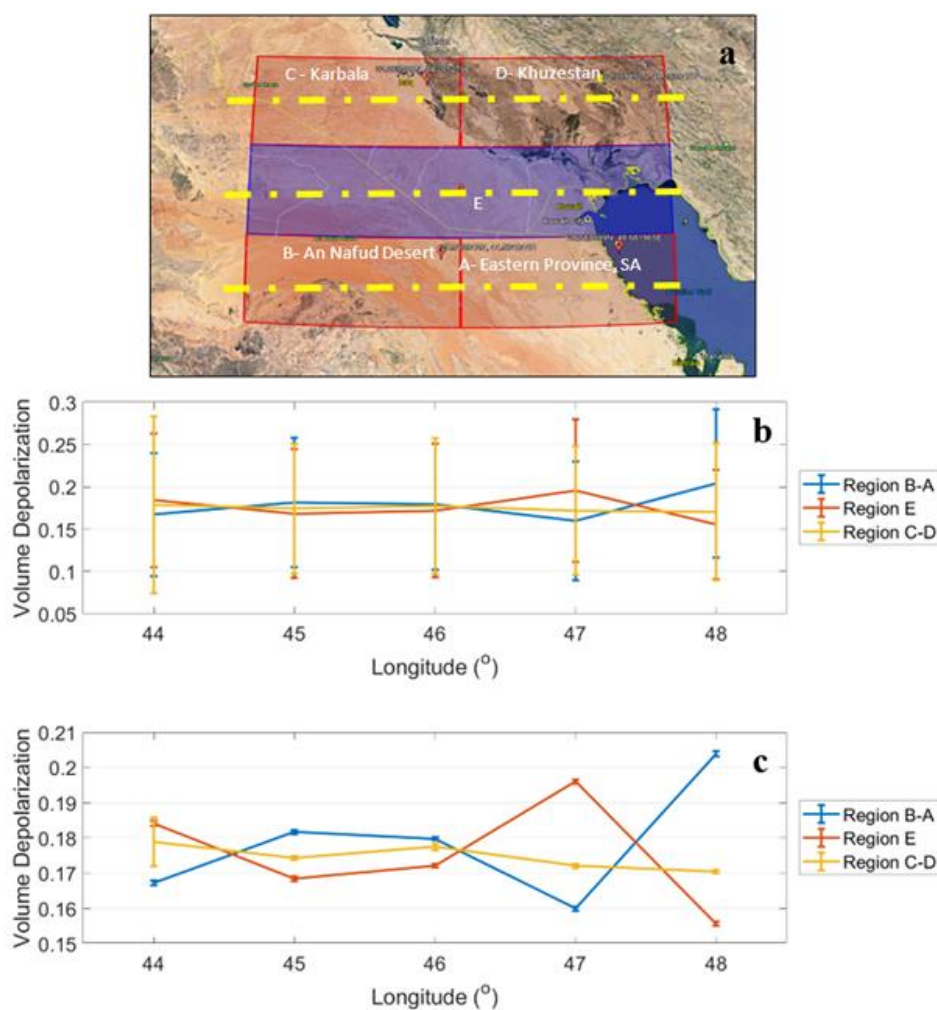
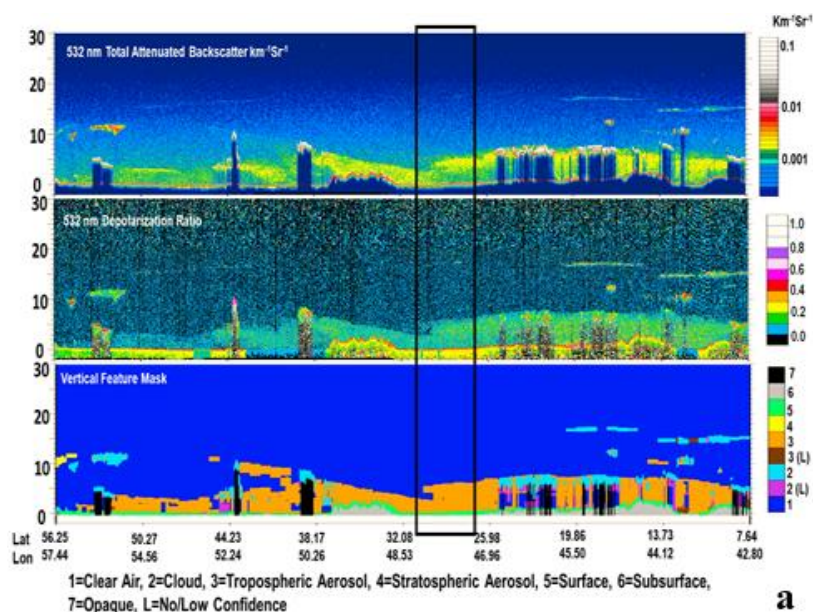


Figure 6. The mean volume depolarization for all dust layers detected below 8 km (a) from June 2006 to April 2019, night and day for the indicated regions (b,c).



MODIS terra RGB, July 8, 2019 (daytime)

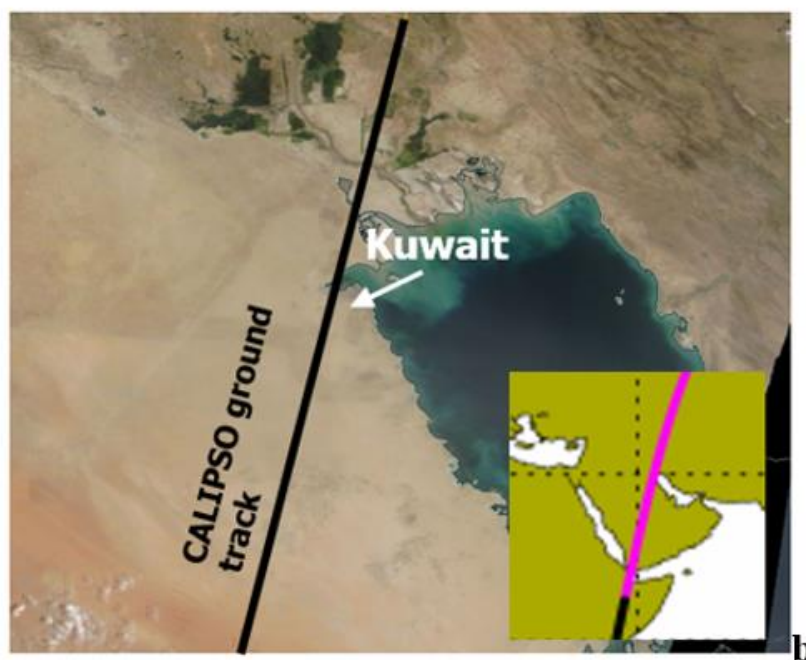


Figure 7. CALIPSO observation on 8 July 2019, at night of a small arrow shape curved SDS type from the area (A) towards Kuwait and the northern Arabian Gulf (a) and the vertical feature mask shows that the dust extended from the surface to a height of ~6 km near Kuwait City (b).

The downwind part (Kuwait) of the two SDS hotspots receives yearly around 373 tons.km^{-2} of fallen dust. The deposited dust downwind of the two hotspots A and B was measured from September to August for two years; in Kuwait, yearly dust levels ranged from 10 to 1065 t/km^2 , with an average of 278 t/km^2 . (Figure 8a,b). According to Safar (1980), Kuwait at downwind of the two hotspots has an annual average of 255.4 dusty days (SDS, rising dust, suspended dust, and haze).

The first year was found to be 43% dustier compared to the second year. The annual SDS days and average within the SDS source area (A) are about 8 and 15 times more in comparison to the downwind and upwind, respectively, from the source (Table 2). The

SDS occasionally occurs more during summer and spring, respectively. The deposited dust annual rates that fall into the Arabian Gulf that originated from the main sources, including the two SDS hotspots, are the highest when compared to all seas and oceans (around 10,330 tons for each cubic kilometer volume of water) [25]. About 40 million people in the region are suffering from the two hotspots, including populations in Iran, Iraq, Kuwait, Bahrain, Saudi, Emirates, and Qatar. Two SDS hotspot locations were identified in the Mesopotamian Flood Plain using 30 years of satellite measurements. Both hotspots encompass roughly 8212 km² and contribute 11%, 42%, 38%, 83%, 85% in 2005, 2012, 2018, 2020, and 2021, respectively, of the total SDS in the region (Figure 9). The SDS originated from the two hotspots that can cover the whole of Arabia and the Arabian Gulf (Figure 10).

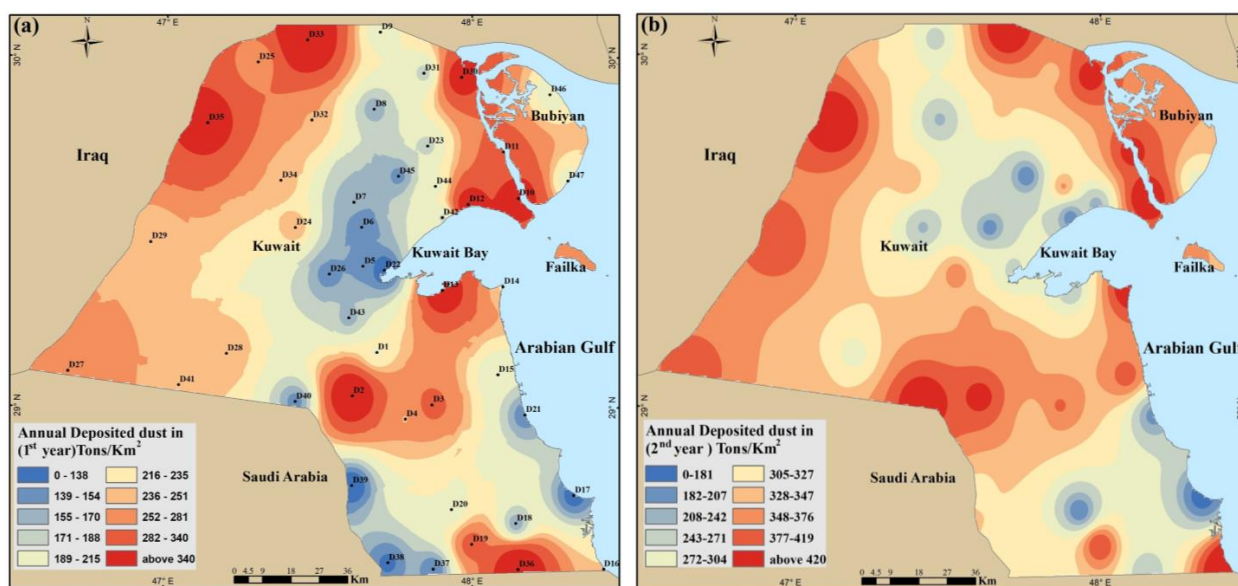


Figure 8. Kuwait annual deposited dust amounts in (tons/km²) for two years from the 1st of September to the 31st of August (a,b).

Table 2. The average number of SDS days in the Middle East hotspot area (A) compared to its surroundings.

Cities	Years	Winter	Spring	Summer	Autumn	Mean Annual
Mosul (Far upwind)	36	1.1	3.6	6.2	3.6	2.1
Baghdad (Upwind)	36	3.7	7.8	10.6	5.5	27.5
Nasiriya (Source area A)	36	3.3	8.8	13.7	5.7	31.5
Kuwait (Downwind)	53	6.0	8.0	11.5	8.4	16.0
Manama (Bahrain)	33	0.5	1.6	3.1	2.0	5.6
Doha (Qatar)	15	1.0	1.8	3.5	2.2	7.6
Abu-Dhabi (Far downwind)	6	1.4	1.1	1.1	0.7	3.9

Comparing results of the Corona Satellite imagery in 1984 and 1991, the reclaimed lands increased through this period from 11,491 km² to 12,824.7 km², while the bare areas decreased to 3649 km² and the waterbody decreased. By comparing the boundaries of the area between 1968 and 1984 (Figure 11), it is clear that the bare lands increased while wetlands decreased due to soil degradation due to the drying up of ponds and swamps and their conversion to agricultural lands. The bare areas between 1984 and 1991 increased in comparison to reclaimed lands, which may be a result of the lack of water in the Mesopotamian Flood Plain region, while the bare land in the years 1991 and 2000 decreased with an increase in the area of cultivated land, which makes its soil vulnerable to

desertification during harvest times, especially in the summer (Figure 11). The bare areas have shrunk significantly, as they decreased in the years 2000, 2013, and 2020 (Figure 11). There is clearly a decrease in bare areas by 1053.2 km² for SDS hotspot (A) and about 1783.1 km² for hotspot (B) (Table 3), due to the increase in the area of cultivated land in 2020. The change series in the total area of the two SDS hotspots during 1968, 1984, 1991, 2000, 2013, and 2020 are illustrated in Figure 12.

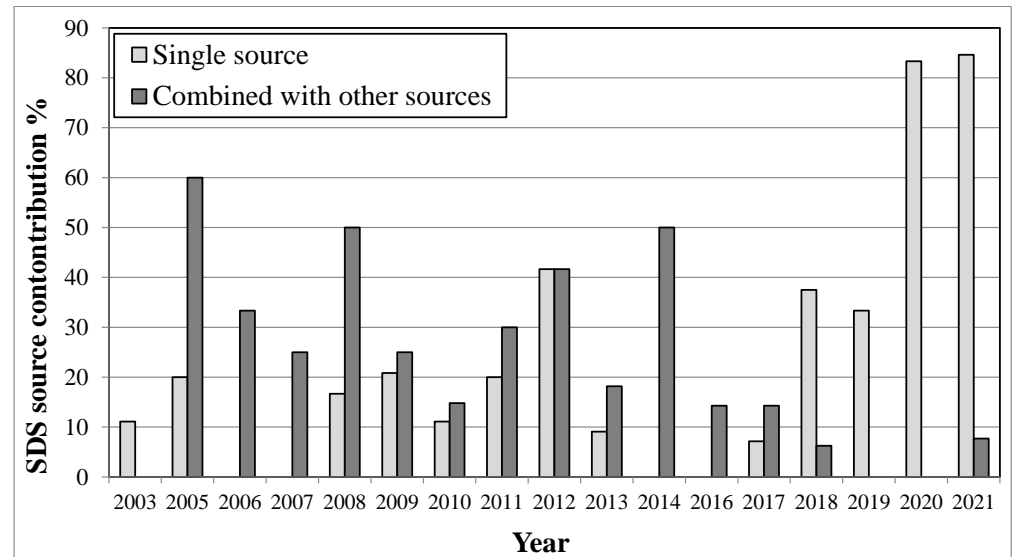


Figure 9. The two SDS hotspots’ contribution percentages in the Middle East as a single source or combined with other sources (2003–2021).

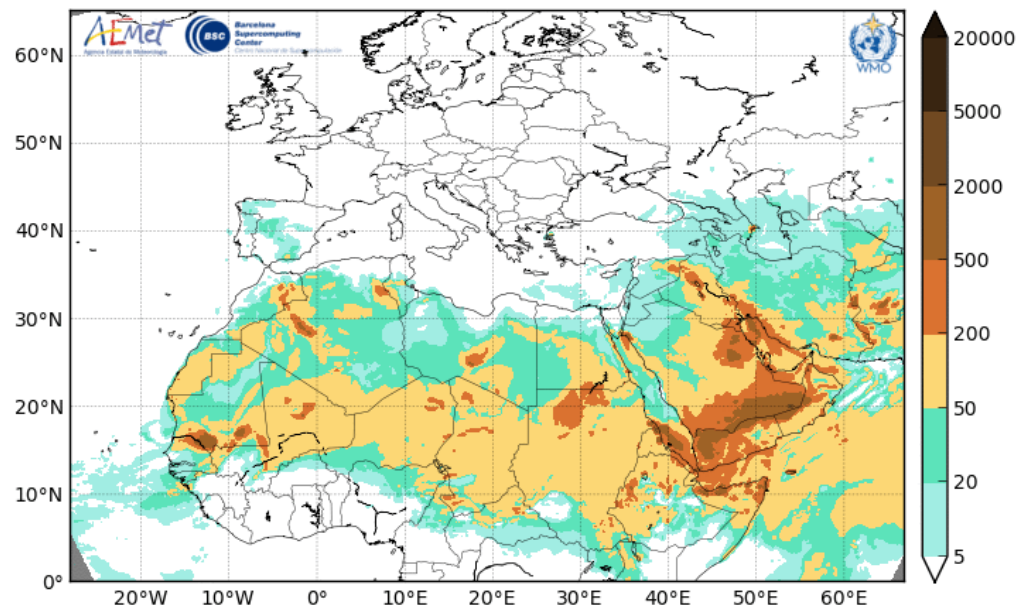


Figure 10. Dust surface concentration image from the Barcelona Dust Forecast Center showing that the SDS on 23 August 2018 originated from the two hotspots affecting the Arabian Gulf and east Arabia.

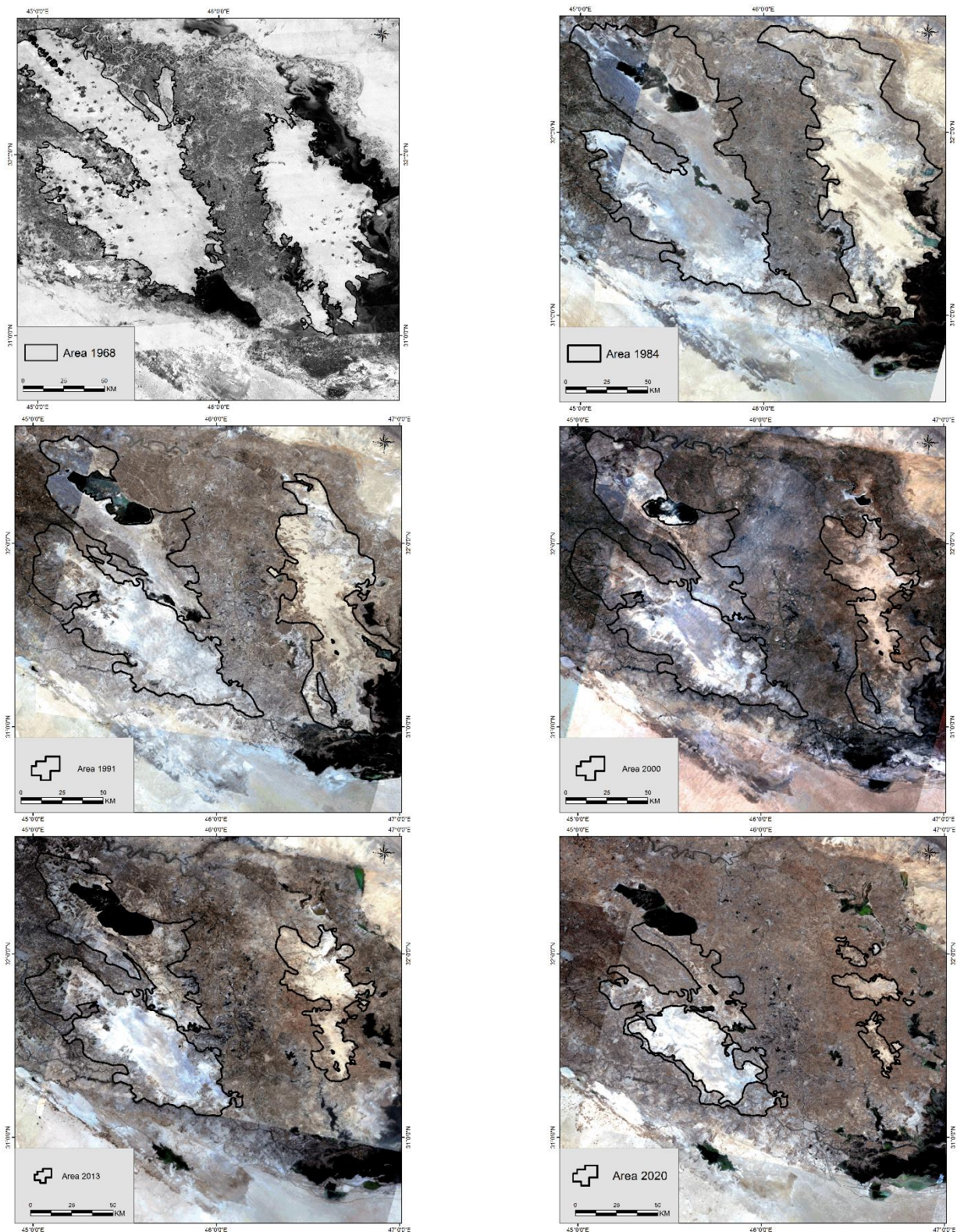


Figure 11. The two studied hotspot areas using Corona Satellite imagery, on 5 May 1968, and Landsat Satellite imagery, on 1984, 1991, 2000, 2013, and 2020.

Table 3. Change in SDS source areas (increase and decrease) with time (1968, 1984, 1991, 2000, 2013, and 2020).

Year	SDS Hotspot-A			Total Changes km ²	SDS Hotspot-B			Total Changes km ²
	Area km ²	Increase km ²	Decrease km ²		Area km ²	Increase km ²	Decrease km ²	
1968	11,491			6512				
1984	12,824.7	3649	2315.4	5964.4	10,506.6	4713	718.8	5431.8
1991	11,499.1	906.4	2232	3138.4	6989.1	392.6	3911.8	4304.4
2000	11,482.7	650.5	666.9	1317.4	4948.4	60	2103.9	2163.9
2013	10,429.5	408	1461.4	1869.4	2964.5	0.0	1983.9	1983.9
2020	6446.6	0.0	3982.9	3982.9	1181.4	0.0	1765.8	1765.8

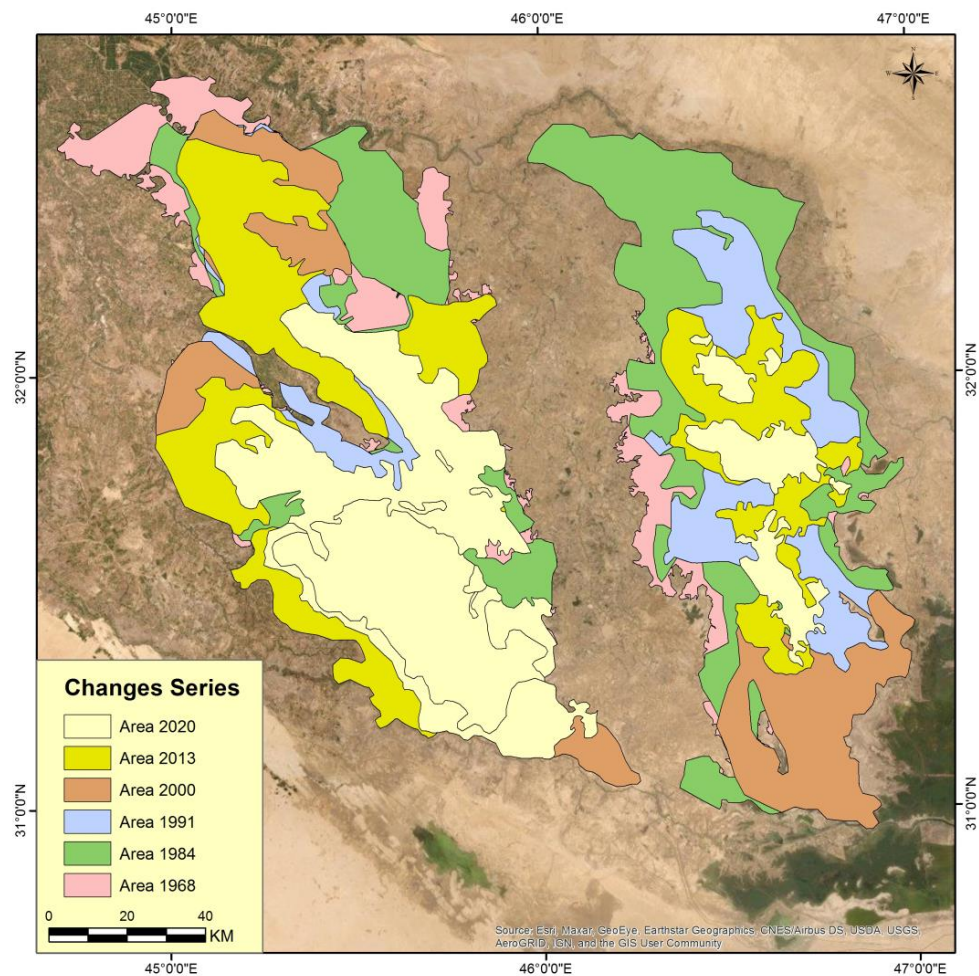


Figure 12. Changes series total area of the two SDS hotspots during 1968, 1984, 1991, 2000, 2013, and 2020.

4.1. The Mineralogical Content

The mineralogy of dust fallout constitutes percentages in the source area compared to upwind and downwind are presented in (Table 4). Quartz, carbonates, and feldspar are the major mineral percentages in deposited dust. Generally, the carbonates ratio is the highest during the spring and winter seasons (October–April). Between October and April, the carbonates in the falling dust in Kuwait increased by up to 58 percent. Carbonates, which make up a large part of the mineralogy of dust fallout, are strong markers of low aeolian activity in the area throughout the winter and spring. Low carbonates percentages in dust, on the other hand, are strong markers of significant aeolian activity throughout

the summer (May–September). Dust in several parts of Kuwait revealed a decrease in carbonate percentages during September. The lowest percentages, down to 5% of the total weight of dust samples, are found in the northern and western regions of the wind corridor. Carbonates in collected dust range from 4 to 36.8% on a yearly basis, with an average of 27.6%. Coastal locations and Kuwait’s northeastern regions have the greatest carbonate percentages. Kuwait dust has almost identical levels of carbonates to that found in nearby regions such as Bahrain and Dubai, but differs significantly from that found in other regional locations, such as Um Qasir and Ahwar-Iraq on Kuwait’s northeastern side (Table 1). This is due to dust storm paths that originate in Iraq and Iran, where carbonates and mud are abundant [26,27].

Table 4. Mean grain size and mineral percentages of deposited dust samples from upwind to downwind in the northern (Tripoli-Libya to Manama-Bahrain) and southern (West Empty Quarter to Dubai-Emirates) Middle East.

Sector	Source	Size Particles %				Semi-Quantitative Mineral %				
		Sand	Mud	Quartz	Calcite	Dolomite	Carbonates	Feldspars	Clay	Others
Northern Middle East										
Tripoli-Libya	[28]	81	20	64	27	0	27	5	4	0
Cairo-Egypt	Present study	90	10	51	20	14	34	15	0	0
Amman-Jordan	Present study	30	70	21	52	16	68	4	0	7
Negev-Palestine	[29]	26	74	41	21	2	23	18	17	0
Baghdad-Mid Iraq	[27]	17	83	49	36	2	38	5	5	3
Um Qasr-SE Iraq	[30]	3	97	13	78	3	80	8	0	0
Kuwait	Present study	37	63	38	38	7	45	10	2	5
Manama-Bahrain	Present study	12	87	32	25	16	41	10	3	15
Southern Middle East										
West Empty Quarter	Present study	40	61	62	13	0	13	24	1	0
East Empty Quarter	Present study	97	4	26	34	19	52	20	1	0
Dubai-Emirates	Present study	17	82	21	25	21	45	6	0	27
Mean		41	59	38	34	9	42	11	3	5
Maximum		97	97	64	78	21	80	24	17	27

The main minerals found in ordinary deposited dust across the world are quartz and carbonates, with feldspars and clay minerals also present in significant quantities. The proportion of quartz varies from 13% in Um Qasr, Iraq, to 64% in Tripoli, Libya, with a national average of 38%. In general, the Middle East’s southern sector (the Empty Quarter region) has greater quartz percentages, whereas the northern sector (around the two hotspot zones) has higher carbonates (varying from 41 to 80 percent) and lower feldspar percentages.

The deposited dust in Iran is with exotic mineralogical content characterized by the lowest carbonate content, (Al, Fe, Mg, and Ca) element oxides, but the highest in (Ba, Cr, and Ni) in comparison to others in the Middle East (Figure 13a). The deposited dust in the SDS hotspot (A) is characterized by high carbonate, but lower than upwind and downwind areas in the Middle East. Additionally, the dust from hotspot (A) and Kuwait shows the lowest in (Ba) compared to other regions in the Middle East (Figure 13b).

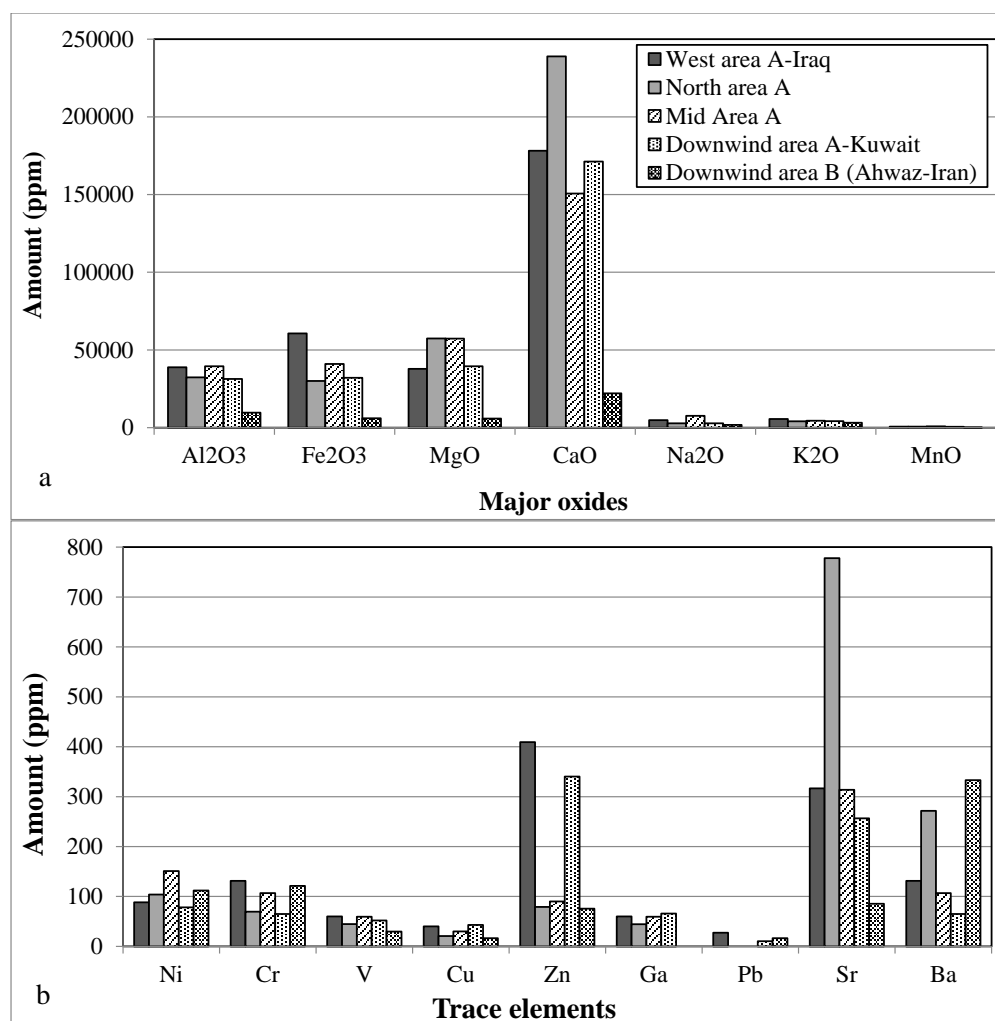


Figure 13. Average major oxides (a) and trace elements (b) for the source area (mid area A) compared to dust collected from upwind (west and north area A) and far downwind (Kuwait and Ahwaz in Iran).

4.2. Radionuclides Analysis

The average activity concentrations of the radionuclides in each country are presented in (Figure 14). The average concentrations of the crustal origin radionuclides, such as ^{40}K , radium, and thorium isotopes, were relatively comparable; however, there is clear evidence that the fallout origin radionuclides (^{210}Pb and ^{137}Cs) concentrations were lower in Tajikistan. In contrast, the primordial radionuclide ^{40}K concentration was the highest compared to the other countries (693 mBq g^{-1}). A multivariate analysis of the radionuclides concentrations and their locations in dust samples was performed (Figure 2a,b) to understand the behavior of the radionuclide in the studied sites. The natural (^{40}K , ^{224}Ra , ^{226}Ra , ^{228}Ra , and ^{234}Th) and the fallout origin radionuclides (^{210}Pb and ^{137}Cs) were well clustered (Figure 2a). ^{137}Cs had been injected into the atmosphere in the mid of the last century via nuclear bomb tests and nuclear power plant accidents (Aba et al., 2018). At the same time, ^{210}Pb is a member of the Uranium series with a half-life time of 22.3 years produced through the decay of the radium subseries in the form of Radon gas. The radon gas exhaled from the soil surface into the air and formed a ^{210}Pb Airborne aerosol. According to geographical and meteorological conditions, both radionuclides will be transported and deposited on the ground at different levels. The resuspension, deposition, and transportation of these radionuclides are complicated processes. Hence, drawing a solid concert statement is tricky, as the results are statistically limited. Even though general conclusions can be

drawn based on (Figures 14 and 15), the relatively low concentrations of ^{210}Pb and ^{137}Cs in Tajikistan samples compared to the other countries might be linked to the different origin and pathways of the dust that impacted the country. In contrast, the other three Middle east countries (Iraq, Kuwait, and Qatar) were clustered in one group, providing that they are vulnerable to similar dust origin and pathways. This conclusion is in line with those obtained by other researchers [31].

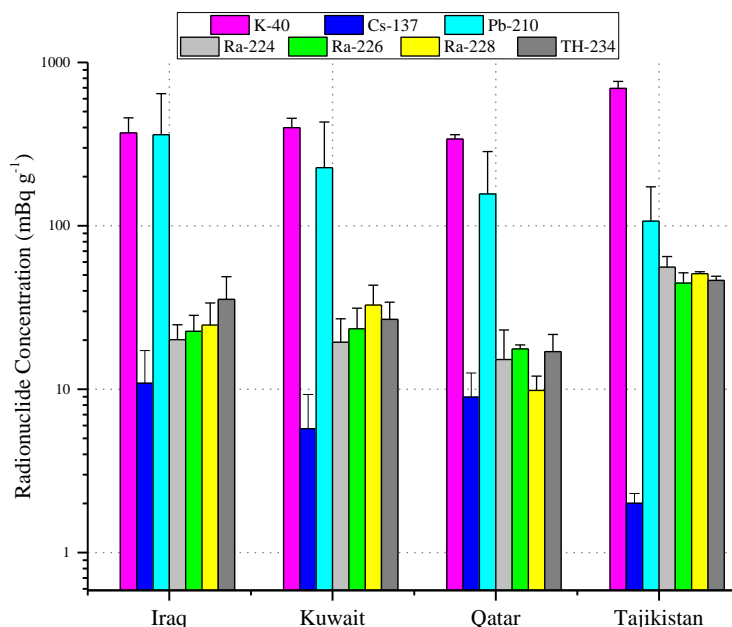


Figure 14. The average concentrations of the radionuclides in dust samples.

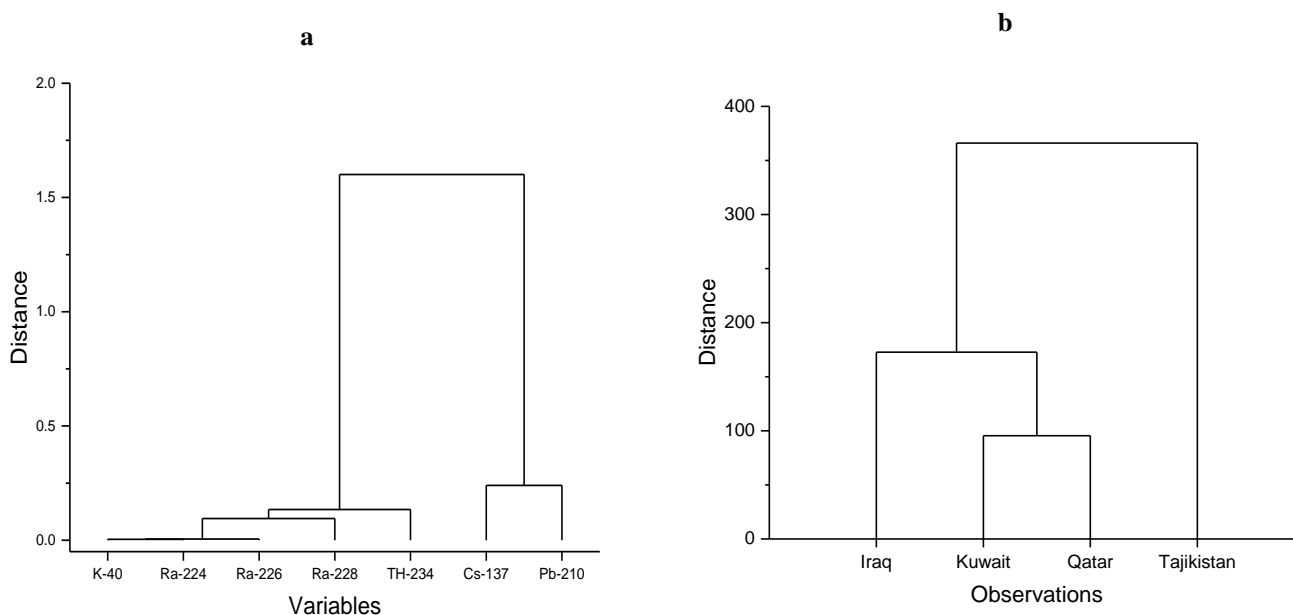


Figure 15. Multivariate analysis of the radionuclide concentrations (a) and their locations (b) in dust samples.

5. Physical Properties

5.1. Particle Size Distribution

Generally, within falling dust, there are two major size portions. Local dust deposition creates relatively coarse dust material larger in diameter than 0.063 mm grain size fractions including very coarse, coarse, fine, and very fine sand fractions, whereas long-distance

transported dust produces fine deposits less than 0.063 mm in size (silt and clay particles) from regional sources. The former form constitutes around 41%, while the latter is 59% (Table 4). The average samples of the surface sediments from the hotspot (A) are poorly sorted, very finely skewed, and platykurtic with dominance of very fine sand (particle diameter between 0.125 mm to 0.063 mm) and mud size portion (32%) (Figure 16). The grain size trimodality may imply multiple sources, which are convenient with the results obtained from the AERONET stations downwind in Kuwait (deposited area). Among all AERONET angstrom results, those SDS that originated from the two hotspots show higher peaks of finer fractions (0.25 μm) compared to other SDS from the western desert of Iraq and Iran. SDS that originate from other sources than the two hotspots are described as unimodal or bimodal with a dominance of 5.5, 4, and 2 μm (Figure 17).

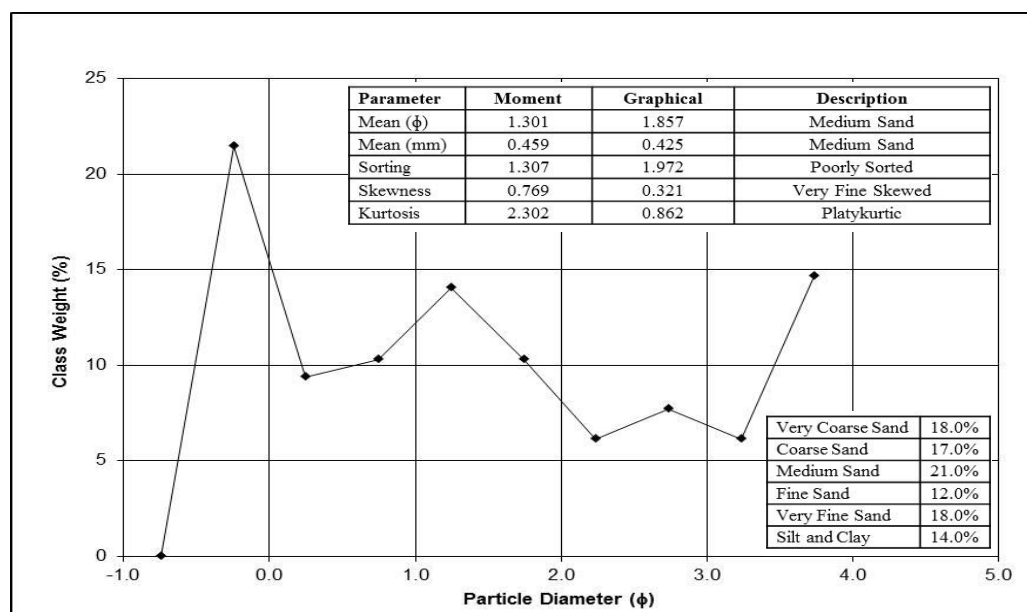


Figure 16. Average histogram and statistical parameters from surface sediments of the hotspot (A), with 32% composed of very fine sand and mud (silt and clay).

The Middle East dust is fine from upwind (Tripoli-Libya) to downwind (Manama-Bahrain) because of the settling of coarse grain size fractions in a short amount of time. The southern Middle East is an outlier, with the main trajectory passing from Iraq’s Western Desert through the Mesopotamian flood plain, which loads the wind with mud size fractions (97%) before heading to Kuwait, Qatar, and Bahrain (desert area), where fallen dust contains 37% sand particles. Sand concentrations were found to be greater in the Rub Khali region of southern Arabia. This is due to the presence of sand dune sea regions and the occurrence of massive sand storms in these two deserts.

Passing through particle size percentages all over the year, some average fallen dust samples from the coastal areas in Kuwait that are located directly downwind of two hotspots show trimodality, which is closely similar to the surface sediments in SDS hotspot (A). There were no temporal but spatial variations observed in the dust particle size percentages and statistical parameters (Figure 18). Western Kuwait shows unimodal particle size distribution which indicates that most of the dust originated from Iraq’s western desert. On the other hand, the coastal areas (Bubiyah island) show trimodality with convenience to those from surface sediments and/or dust collected after SDS from the hotspot (A).

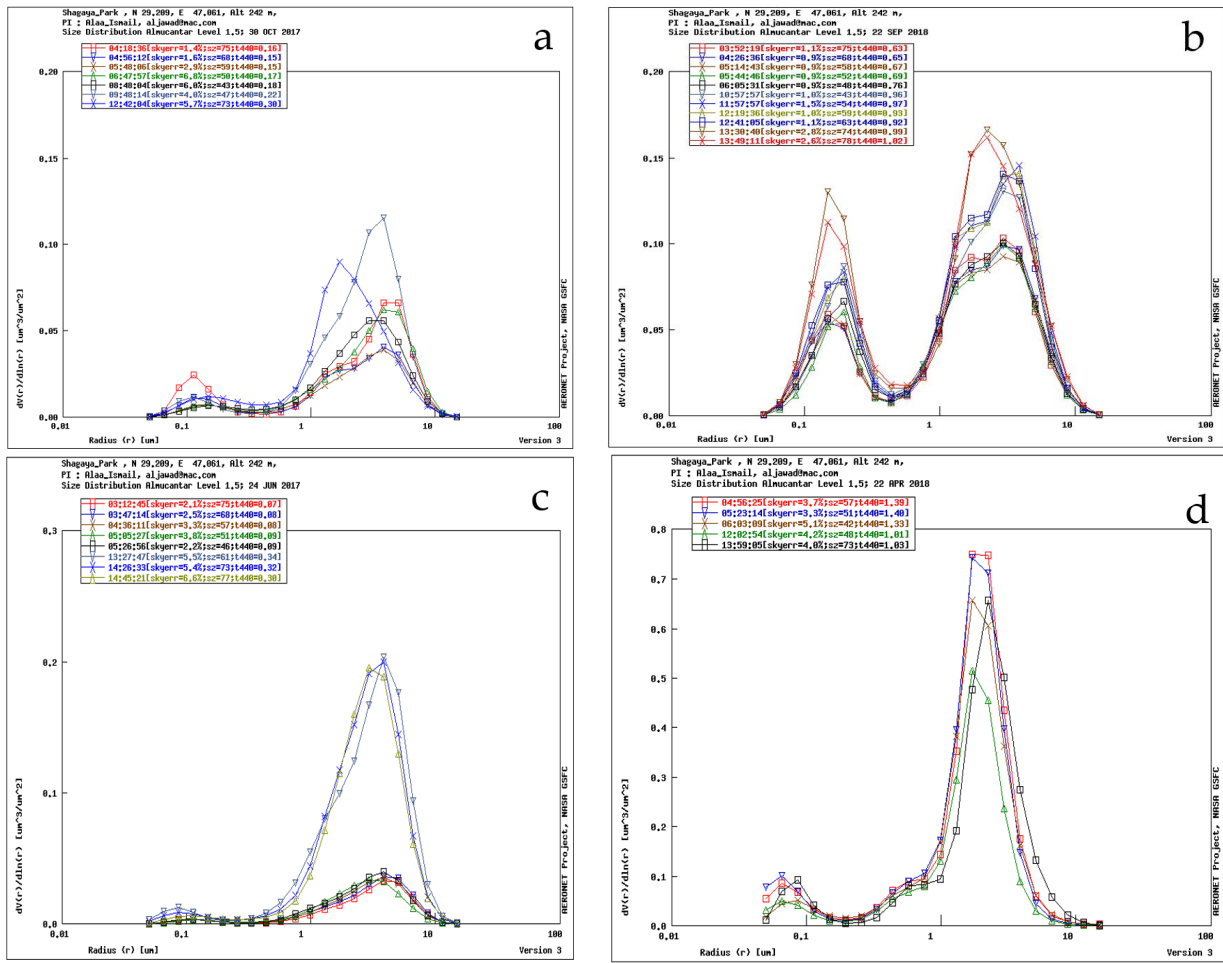


Figure 17. A trimodal AOT/Angstrom for sand and dust storms (SDS) of three combined sources, mostly from the Mesopotamian Flood Plain (a), from the two hotspots (b), characterized by a high peak at 0.25 μm , and the Western Desert of Iraq (c,d).

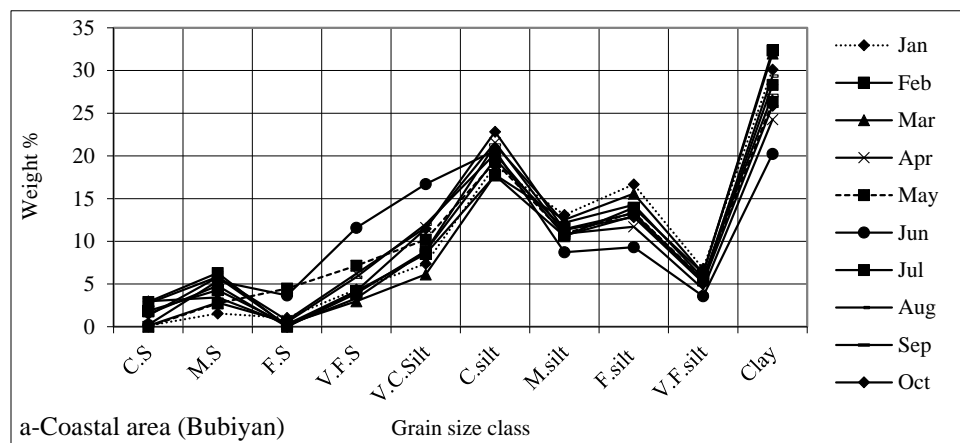


Figure 18. Cont.

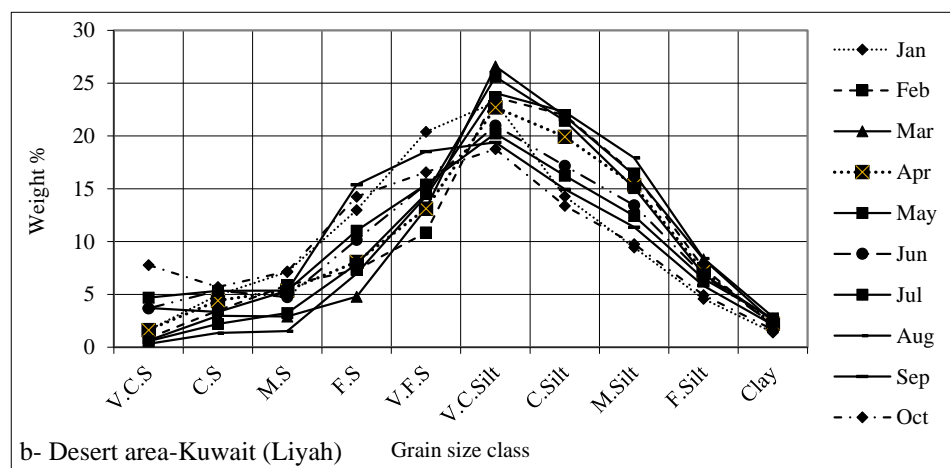


Figure 18. Temporal variations of grain size percentages of dust in Kuwait within the coastal (a) and the desert (b) areas downwind from the two SDS hotspots. (V.C.S.: Very Coarse sand; C.S.: Coarse sand; M.S.: Medium sand; F.S.: Fine sand; V.F.S.: Very fine sand; V.C.Silt.: Very coarse silt; C. Silt: Coarse silt; M.Silt: Medium silt; F.Silt: Fine silt; V.F.Silt: Very fine silt).

5.2. BET Surface Area

The BET surface area for collected deposited dust of 26 locations from far upwind (Sabha-Libya) passing through the hotspot area (A) into far downwind (Ain-Emirates) was analyzed. Additionally, the assessment was stretched to cover global and regional dust samples.

The dust samples collected from SDS hotspot B had surface area values that were quite variable from global and regional dust samples. The BET surface area from far upwind (Libya, Egypt, Palestine, and Jordan) are the lowest in comparison to all collected dust samples. Dust samples from the Mesopotamian Flood plain and the hotspot area (A) show the highest BET surface area, due to the sedimentological and geographical characteristics. The BET surface area values with global and regional dust particles demonstrate higher variability for global dust particles in Cartagena-Colombia and regional particles (Amman-Jordan and Cairo-Egypt) but are similar to dust samples collected from Arabian Gulf countries (Figure 19). The research region’s surface area varies throughout time, indicating various origins. The dust in coastal areas is shifted from multi-regional sources, but predominantly from the Mesopotamian Flood plain (Figure 19) and partially from the African Desert, the western desert of Iraq, and the northern desert of Arabia.

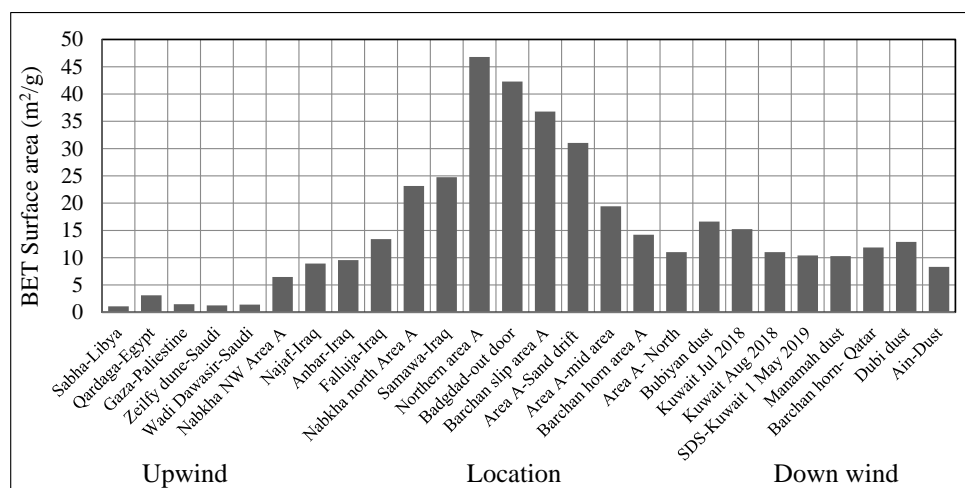


Figure 19. The dust BET surface area in the hotspot (A) compared to up- and downwind collected dust samples.

6. Planned Control Measures

Treating shifting sand and suspended dust reduces the chances of SDS occurring from major sources (the two hotspots), which directly enhance health and social activities in the downwind regions (Southern Iraq, Ahwaz-Iran, Kuwait, and other gulf countries). Therefore, a four-year plan project will be implemented by the Kuwait Institute for Scientific Research (KISR), with a total cost of 21 million US dollars, to put control plans for hotspot (B) as it acts as the major source of SDS in southern Iraq. The activities that will be implemented to address the challenge will include:

Afforestation: Green belts and windbreaks using native plants (*Tamarix artaculata*, *Atriplex halimus*) and drought-resistant trees (*Prosopis juliflora*) will be constructed and planted in the form of tapes to reduce wind action and give durability to treatment. Preparing seedlings of trees and shrubs, it is required to establish a specialized nursery for a production capacity estimated at 1–2 million seedlings per year, with the provision of the requirements for establishing the nursery, including wooden and plastic canopies, seeds, cuttings, plastic bags, employment of 20 workers, watering requirements, and transporting seedlings to afforestation sites. Providing water to afforestation sites is necessary, and water sources for irrigation will be drained via establishing channels from the main rivers within the general plan for the project duration (Figure 20).

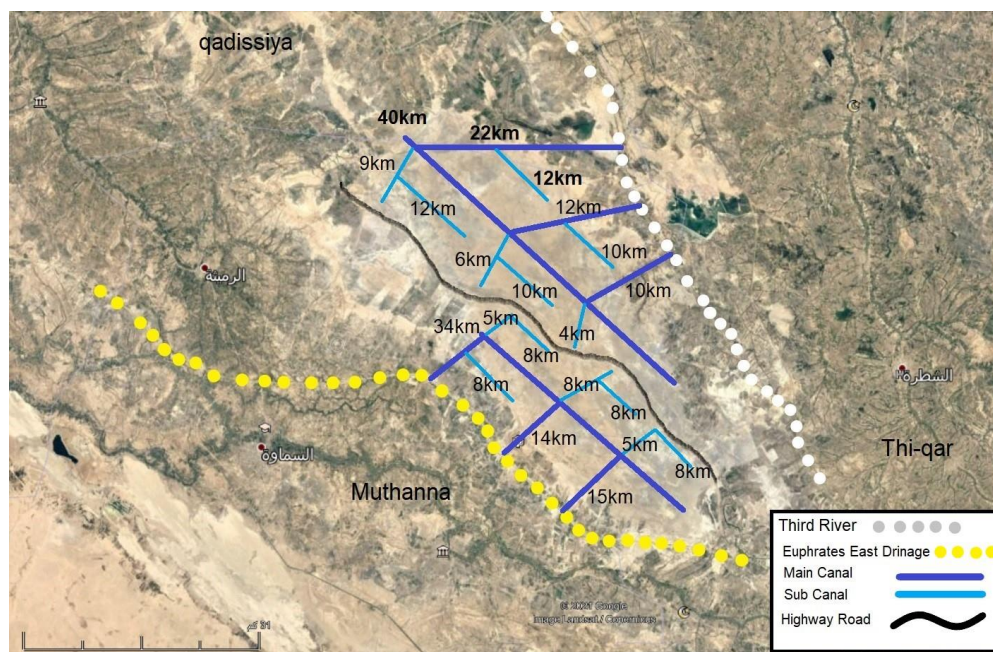


Figure 20. The general plan for draining channels from main streams and rivers for SDS hotspot (A).

Mud coverage: through the use of heavy machinery (bulldozers and shafts), a layer of 25 cm thickness is placed to cover the present sand dunes in both hotspots, where the mud acts as heavy soils that hold together when rain falls, which reduces the chances of their movement by the wind, and thus, allows growth for native plants.

7. Conclusions

Two source locations (hotspots) for SDS in the southern part of the Mesopotamian Flood Plain were identified as hotspot areas (A) and (B). Both hotspots encompass roughly 5356 km² and contribute 11% in 2005 to 85% in 2021 of the total SDS in the region. Both SDS hotspot areas are decreasing with time. Area (B) is covered by farms and cultivation and is expected to be completely stabilized by the end of 2022. On the other hand, area (A) acts as a major source of sand and dust storms. Therefore, a plan was put in action involving satellite remote sensing and robust transport models to locate the most effective sites for planting can be used to develop an effective reforestation strategy for this hotspot.

The plan will include dredging channels and attributes from major rivers and water bodies covering the area to stabilize the SDS hotspot. The vertical distribution of dust plumes was regularly observed by the CALIPSO downwind of the two hotspots. The vertical feature mask shows that the dust extended from the surface to a height of ~6 km near Kuwait City. The evolution of microphysical properties of the dust was tracked using volume depolarization ratio and was found to increase with the longitude, indicating a gradual change in the dust properties as they are transported westwards.

Passing through particle size percentages all over the year, some average fallen dust samples from the coastal areas in Kuwait that are located directly downwind of two hotspots show trimodality, which is similar to the surface sediments in SDS hotspot (A). The natural (^{40}K , ^{224}Ra , ^{226}Ra , ^{228}Ra , and ^{234}Th) and the fallout origin radionuclides (^{210}Pb and ^{137}Cs) were well clustered. In contrast, the other three Middle East countries (Iraq, Kuwait, and Qatar) were clustered in one group, providing that they are vulnerable to similar dust origin and pathways. On the other hand, the two hotspots (A and B) are characterized by the highest BET surface area for dust particles in comparison to all collected samples all over the world. The BET surface area for dust particles is decreasing with distance from all directions from the two hotspots (A and B). This can be attributed due to the high content of carbonates and clay minerals, which was reflected in the major and trace element quantities.

More research should be done on adapting to SDS by regulating or redirecting sand grain particles, which account for almost one-third of the overall dust percentages, particularly in desert regions. Additionally, more mitigation plans should be implemented around the affected urban areas in the region.

Author Contributions: A.A.-D. designed this research; A.O., A.A. (Abdulaziz Aba), M.A. (Majid Alrashedi), O.B., M.J., N.A.-D., T.W. and A.E. performed data analyses; A.A. (Abdulaziz Aba), M.A. (Mohamad Alrawi), M.A. (Modi Ahmed), P.P. and A.O. performed model simulations; A.A. (Abeer Alsaleh), A.O., A.R. and M.J. made contributions to discussion; A.A.-H., A.O. and A.R. wrote the paper. All authors have read and agreed to the published version of the manuscript.

Funding: The Kuwait Institute for Scientific Study (KISR) and the Kuwait Foundation for Advancement of Science (KFAS) grant number: 2008-1401-01.

Institutional Review Board Statement: Not applicable.

Informed Consent Statement: Not applicable.

Data Availability Statement: The data presented in this study are available upon request from the corresponding author.

Acknowledgments: The Kuwait Institute for Scientific Study (KISR) and the Kuwait Foundation for Advancement of Science (KFAS) are highly appreciated for financing the research dust project-EC063C grant number: 2008-1401-01 and permitting the manuscript's publication. Our appreciation to Kuwait Meteorological Centers in Kuwait, Bahrain, Qatar, and Emirates for supporting meteorological data.

Conflicts of Interest: The authors declare that they have no known competing financial interest or personal relationships that could have appeared to influence the work reported in this paper.

References

1. Mohammadpour, K.; Rashki, A.; Sciortino, M.; Kaskaoutis, D.G.; Bolorani, A.D. A statistical approach for identification of dust-AOD hotspots climatology and clustering of dust regimes over Southwest Asia and the Arabian Sea. *Atmospheric Pollut. Res.* **2022**, *13*, 101395. [[CrossRef](#)]
2. Doronzo, D.M.; Al-Dousari, A.; Folch, A.; Dagsson-Waldhauserova, P. Preface to the Dust Topical Collection. *Arab. J. Geosci.* **2016**, *9*, 468. [[CrossRef](#)]
3. Al-Dousari, A.; Pye, K.; Al-Hazza, A.; Al-Shatti, F.; Ahmed, M.; Al-Dousari, N.; Rajab, M. Nanosize inclusions as a fingerprint for aeolian sediments. *J. Nanopart. Res.* **2020**, *22*, 94. [[CrossRef](#)]
4. Rashki, A.; Kaskaoutis, D.G.; Sepehr, A. Statistical evaluation of the dust events at selected stations in Southwest Asia: From the Caspian Sea to the Arabian Sea. *CATENA* **2018**, *165*, 590–603. [[CrossRef](#)]

5. Al-Ghadban, A.N.; Saeed, T.; Al-Dousari, A.; Al-Shemmari, H.; Al-Mutairi, M. Preliminary assessment of the impact of draining of Iraqi marshes on Kuwait's northern marine environment. Part I. Physical manipulation. *Water Sci. Technol.* **1999**, *40*, 75–87. [[CrossRef](#)]
6. Subramaniam, N.; Al-Sudairawi, M.; Al-Dousari, A.; Al-Dousari, N. Probability distribution and extreme value analysis of total suspended particulate matter in Kuwait. *Arab. J. Geosci.* **2015**, *8*, 11329–11344. [[CrossRef](#)]
7. Neelamani, S.; Al-Dousari, A. A study on the annual fallout of the dust and the associated elements into the Kuwait Bay, Kuwait. *Arab. J. Geosci.* **2016**, *9*, 210. [[CrossRef](#)]
8. Bolorani, A.D.; Samany, N.N.; Papi, R.; Soleimani, M. Dust source susceptibility mapping in Tigris and Euphrates basin using remotely sensed imagery. *Catena* **2022**, *209*, 105795. [[CrossRef](#)]
9. Rashki, A.; Kaskaoutis, D.; Rautenbach, C.; Eriksson, P.; Qiang, M.; Gupta, P. Dust storms and their horizontal dust loading in the Sistan region, Iran. *Aeolian Res.* **2012**, *5*, 51–62. [[CrossRef](#)]
10. Al-Dousari, A.M.; Ibrahim, M.I.; Al-Dousari, N.; Ahmed, M.; Al-Awadhi, S. Pollen in aeolian dust with relation to allergy and asthma in Kuwait. *Aerobiologia* **2018**, *34*, 325–336. [[CrossRef](#)]
11. Faridi, S.; Brook, R.D.; Yousefian, F.; Hassanvand, M.S.; Nodehi, R.N.; Shamsipour, M.; Rajagopalan, S.; Naddafi, K. Effects of respirators to reduce fine particulate matter exposures on blood pressure and heart rate variability: A systematic review and meta-analysis. *Environ. Pollut.* **2022**, *303*, 119109. [[CrossRef](#)]
12. Sofiev, M.; Winebrake, J.J.; Johansson, L.; Carr, E.; Prank, M.; Soares, J.; Vira, J.; Kouznetsov, R.; Jalkanen, J.-P.; Corbett, J.J. Cleaner fuels for ships provide public health benefits with climate tradeoffs. *Nat. Commun.* **2018**, *9*, 406. [[CrossRef](#)]
13. Al-Dousari, A.M. Causes and indicators of land degradation in the north-western part of Kuwait. *Arab. Gulf J. Sci. Res. (1989)* **2005**, *23*, 69–79.
14. Middleton, N.; Kashani, S.S.; Attarchi, S.; Rahnama, M.; Mosalman, S.T. Synoptic Causes and Socio-Economic Consequences of a Severe Dust Storm in the Middle East. *Atmosphere* **2021**, *12*, 1435. [[CrossRef](#)]
15. Al-Awadhi, J.M.; Al-Dousari, A.; Al-Enezi, A. Barchan dunes in northern Kuwait. *Arab. Gulf J. Sci. Res.* **2000**, *18*, 32–40.
16. Alshemmari, H.; Al-Dousari, A.M.; Talebi, L.; Al-Ghadban, A.N. Mineralogical characteristics of surface sediment in Sulaibikhat Bay, Kuwait. *Kuwait J. Sci.* **2013**, *40*, 159–176.
17. Al-Dousari, A.M.; Alsaleh, A.; Ahmed, M.; Misak, R.; Al-Dousari, N.; Al-Shatti, F.; Elrawi, M.; William, T. Off-road vehicle tracks and grazing points in relation to soil compaction and land degradation. *Earth Syst. Environ.* **2019**, *3*, 471–482. [[CrossRef](#)]
18. Al-Dousari, A.; Ramadan, A.; Al-Qattan, A.; Al-Ateeqi, S.; Dashti, H.; Ahmed, M.; Al-Dousari, N.; Al-Hashash, N.; Othman, A. Cost and effect of native vegetation change on aeolian sand, dust, microclimate and sustainable energy in Kuwait. *J. Taibah Univ. Sci.* **2020**, *14*, 628–639. [[CrossRef](#)]
19. Al-Hemoud, A.; Al-Dousari, A.; Al-Dashti, H.; Petrov, P.; Al-Saleh, A.; Al-Khafaji, S.; Behbehani, W.; Li, J.; Koutrakis, P. Sand and dust storm trajectories from Iraq Mesopotamian flood plain to Kuwait. *Sci. Total Environ.* **2019**, *710*, 136291. [[CrossRef](#)]
20. Yassin, M.F.; Almutairi, S.K.; Al-Hemoud, A. Dust storms backward Trajectories' and source identification over Kuwait. *Atmospheric Res.* **2018**, *212*, 158–171. [[CrossRef](#)]
21. Safar, M.I. *Frequency of Dust in Daytime Summer in Kuwait*; Meteorological Department, Directorate General of Civil Aviation: Kuwait City, Kuwait, 1980. (In Arabic)
22. Rott, C. Saharan Sand and Dust—Characterization, Deposition Rates and Implications. Master's Thesis, Royal Holloway University of London, Egham, UK, 2001.
23. Reheis, M. A 16-year record of eolian dust in Southern Nevada and California, USA: Controls on dust generation and accumulation. *J. Arid Environ.* **2006**, *67*, 487–520. [[CrossRef](#)]
24. Hoffmann, C.; Funk, R.; Sommer, M.; Li, Y. Temporal variations in PM10 and particle size distribution during Asian dust storms in Inner Mongolia. *Atmos. Environ.* **2008**, *42*, 8422–8431. [[CrossRef](#)]
25. Al-Dousari, A.; Doronzo, D.; Ahmed, M. Types, Indications and Impact Evaluation of Sand and Dust Storms Trajectories in the Arabian Gulf. *Sustainability* **2017**, *9*, 1526. [[CrossRef](#)]
26. Attiya, A.A.; Jones, B.G. Assessment of mineralogical and chemical properties of airborne dust in Iraq. *SN Appl. Sci.* **2020**, *2*, 1614. [[CrossRef](#)]
27. Awadh, S.M. Geochemistry and mineralogical composition of the airborne particles of sand dunes and dust storms settled in Iraq and their environmental impacts. *Environ. Earth Sci.* **2011**, *66*, 2247–2256. [[CrossRef](#)]
28. O'Hara, S.L.; Clarke, M.L.; Elatrash, M.S. Field measurements of desert dust deposition in Libya. *Atmos. Environ.* **2006**, *40*, 3881–3897. [[CrossRef](#)]
29. Crouvi, O.; Amit, R.; Enzel, Y.; Porat, N.; Sandler, A. Sand dunes as a major proximal dust source for late Pleistocene loess in the Negev Desert, Israel. *Quat. Res.* **2008**, *70*, 275–282. [[CrossRef](#)]
30. Gharib, I.; Al-Hashash, M.; Anwar, M. *Dust Fallout in Northern Part of the ROPME Sea Area*; Report No. KISR2266; Kuwait Institute for Scientific Research: Kuwait City, Kuwait, 1987.
31. Aba, A.; Al-Dousari, A.; Ismaeel, A. Atmospheric deposition fluxes of ¹³⁷Cs associated with dust fallout in the northeastern Arabian Gulf. *J. Environ. Radioact.* **2018**, *192*, 565–572. [[CrossRef](#)]